

Cortical Local Field Potential Encodes Movement Intentions in the Posterior Parietal Cortex

Hansjörg Scherberger,^{1,2,*} Murray R. Jarvis,¹
and Richard A. Andersen¹

¹Division of Biology
California Institute of Technology
Pasadena, California 91125

Summary

The cortical local field potential (LFP) is a summation signal of excitatory and inhibitory dendritic potentials that has recently become of increasing interest. We report that LFP signals in the parietal reach region (PRR) of the posterior parietal cortex of macaque monkeys have temporal structure that varies with the type of planned or executed motor behavior. LFP signals from PRR provide better decode performance for reaches compared to saccades and have stronger coherency with simultaneously recorded spiking activity during the planning of reach movements than during saccade planning. LFP signals predict the animal's behavioral state (e.g., planning a reach or saccade) and the direction of the currently planned movement from single-trial information. This new evidence provides further support for a role of the parietal cortex in movement planning and the potential application of LFP signals for a brain-machine interface.

Introduction

The cortical local field potential (LFP) has long been known as a summation signal of excitatory and inhibitory dendritic potentials in a “listening sphere” around the tip of the electrode (Buzsaki, 2004; Fromm and Bond, 1964; Gray et al., 1989; Mitzdorf, 1987). In the last few years, the LFP signal has received increasing attention for a number of reasons. First, the temporal structure of the LFP has been shown to reflect sensory and motor-related signals that can be modulated by cognitive processes. The LFP therefore provides additional information to single neuron activity (Fries et al., 2001; Mehring et al., 2003; Pesaran et al., 2002; Sanes and Donoghue, 1993). Second, the source of LFPs is largely from synaptic activity, whereas action potentials recorded from conventional microelectrodes are generally from large pyramidal cells. Thus, LFPs and spikes recorded from the same sites tend to represent different sources—the LFPs represent the inputs and local processing, and the spikes represent the outputs (Mitzdorf, 1987). Third, LFPs appear to be more closely correlated than spikes with the BOLD signal recorded in fMRI (Buzsaki, 2004; Logothetis et al., 2001; Logothetis and Wandell, 2004). Fourth, spiking activity has been shown to cohere with the LFP under certain be-

havioral or perceptual conditions, which potentially can provide new evidence regarding the functional organization of the underlying neuronal networks (Engel et al., 1990; Fries et al., 2001; Murthy and Fetz, 1996; Siegel and Konig, 2003). Finally, the cortical LFP is easy to record, even over long periods of time, which could be of practical use for the development of reliable brain-machine interfaces, e.g., as needed for a neural prosthesis (Andersen et al., 2004).

In the present study, we report the coding properties of the LFP, spiking activity, and the coherence between the LFP and spiking activity in the parietal reach region (PRR) of the posterior parietal cortex (PPC) of macaque monkeys during the planning and execution of reach movements and saccades. This region has been shown to play an important role in the sensorimotor transformations for the planning of arm reach movements (Andersen et al., 1997; Batista et al., 1999; Buneo et al., 2002; Mountcastle et al., 1975; Scherberger and Andersen, 2003; Snyder et al., 1997). We find considerable differences in the temporal structure of the LFP and the spike-field coherence when monkeys planned and executed reaches and saccades, and the LFP was tuned for the planned reach direction. Furthermore, this information could be decoded on a trial-by-trial basis from simulated population activity of the LFP. This new evidence provides further support for a role of parietal cortex in movement planning.

Results

To compare the properties of LFP and of spiking activity in PRR during the planning and execution of reach and saccade movements, two macaque monkeys were trained to perform a delayed arm reaching task and a delayed saccade task (Figure 1A). In each trial, the animal first fixated and touched a central fixation spot (baseline), before a visual cue was presented at one of eight possible target positions. Depending on the color of the presented cue, the animal then planned to reach (green cue) or saccade (red cue) to the target but had to withhold movement execution until the fixation light was extinguished. Figures 1C–1H show the neural activity of one typical PRR recording site in these two tasks. In accordance with previous reports (Batista et al., 1999; Snyder et al., 1997; Snyder et al., 2000), spiking activity during the reach task increased after the cue was presented and stayed elevated during the planning period until the movement was executed (Figure 1C). During the saccade task, spiking activity was only moderately elevated (Figure 1D).

Spectrograms of simultaneously recorded LFP signals from the same site revealed a change in the LFP power spectrum during the reach task after the cue was presented. The power at frequencies below 15 Hz decreased strongly, while the power in the frequency band 15–40 Hz increased (Figure 1E). In contrast, the spectrogram of this recording site showed only moderately increased power at low frequencies (0–15 Hz) but not

*Correspondence: hjs@ini.phys.ethz.ch

²Present address: Institute of Neuroinformatics, ETH and University of Zürich, CH-8057 Zürich, Switzerland.

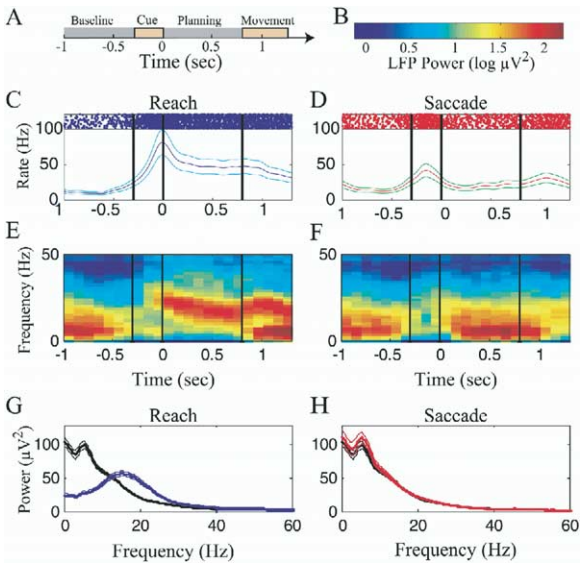


Figure 1. Neural Signals from a Typical Site

(A) Temporal evolution of the behavioral tasks. (C and D) Spike rasters and peristimulus time histograms including 95% confidence limits of spiking activity during the delayed reach and delayed saccade task. (E and F) Spectrogram of the simultaneously recorded LFP activity. Color legend shown in (B). Vertical bars: begin and end of the cue and planning periods. (G and H) LFP spectrum during the baseline (black lines) and planning period of the reach (blue line) and saccade task (red line). Thin lines indicate 95% confidence limits.

at higher frequencies during the saccade task (Figure 1F). The spectra of the LFP in the planning period (Figures 1G and 1H) indicate that these changes are significant. Clearly, for this site, the temporal structure of the LFP depends on the type of planned and executed motor behavior.

These findings were confirmed by a population analysis of 119 sequentially recorded sites. Figure 2A shows the mean LFP spectrum for the population on a logarithmic scale normalized by the LFP activity during the baseline period (horizontal zero line). During reach planning, we found that the mean LFP power of the population was significantly lower than the baseline LFP spectrum at frequencies below 10 Hz and significantly larger than baseline at frequencies of 10–100 Hz. During saccade planning, the LFP power was moderately elevated in the frequency range 1–100 Hz. This confirms the presence of different temporal structure for different motor plans in the population. During movement execution (Figure 2B), the mean LFP power during reaching was significantly larger than baseline at frequencies up to 100 Hz except for a small dip around 10 Hz that appeared no different from baseline. In contrast, the LFP spectrum during saccade execution showed only moderate deviations from baseline.

LFP spectra of individual recording sites showed a high degree of discriminability between time intervals of reach and saccade planning and execution. To quantify the differences between the reach and saccade LFP spectra, we calculated for each recording site a discrimi-

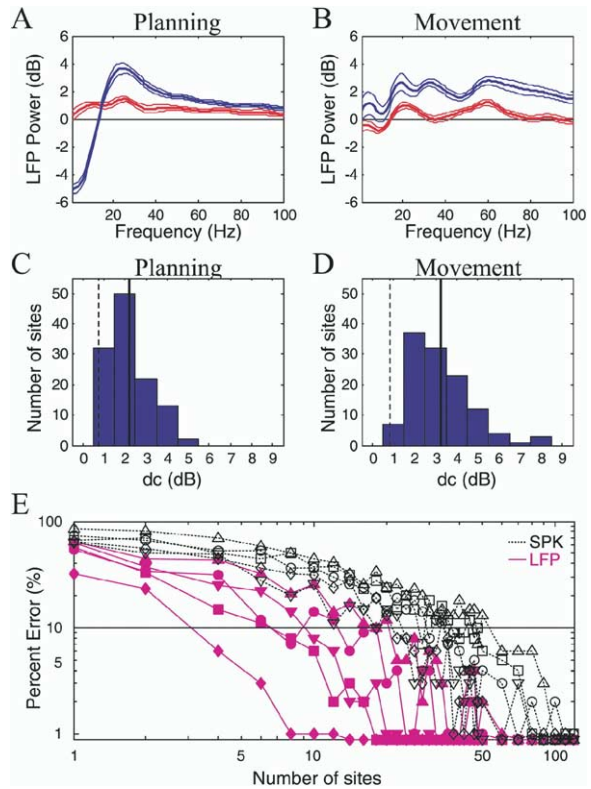


Figure 2. LFP Spectra during Movement Planning and Execution

(A and B) LFP spectrum of the population during planning and execution of reach and saccade movements. LFP power is given in decibels relative to baseline activity. Thin lines indicate standard error.

(C and D) Histogram of discriminability coefficient (dc) between reach and saccade spectra over all recording sites. Solid vertical line, mean; dotted line, significance level $p = 0.001$.

(E) Decoding predictability of the animal's behavioral states from the LFP (red) and spiking activity (black) using Bayesian classification as a function of the number of recording sites (both axes on a log scale). Behavioral states indicated by markers: baseline (circles), reach planning (squares) and execution (diamonds), saccade planning (upward-pointing triangles) and execution (downward-pointing triangles). Horizontal line, 10% error level.

nability coefficient (dc) that describes the average discriminability between the reach and saccade spectra at frequencies 1–100 Hz (see Experimental Procedures). Using this measure, we found a mean dc value of 2.18 dB for movement planning and of 3.26 dB for movement execution (vertical solid lines in Figures 2C and 2D), which significantly exceeded the 0.1% error lines for the hypothesis of identical spectra (vertical dotted lines in Figures 2C and 2D). These findings confirm different LFP spectra in PRR for the planning and execution of reach movements and saccades.

To compare the coding of the behavioral state in the LFP signals and in spiking activity, we explored how well the behavioral state of the animal (baseline, reach planning, saccade planning, reach movement, saccade movement) could be predicted from our data set. For this, we treated our data set of sequentially recorded sites as if it were simultaneously acquired and pre-

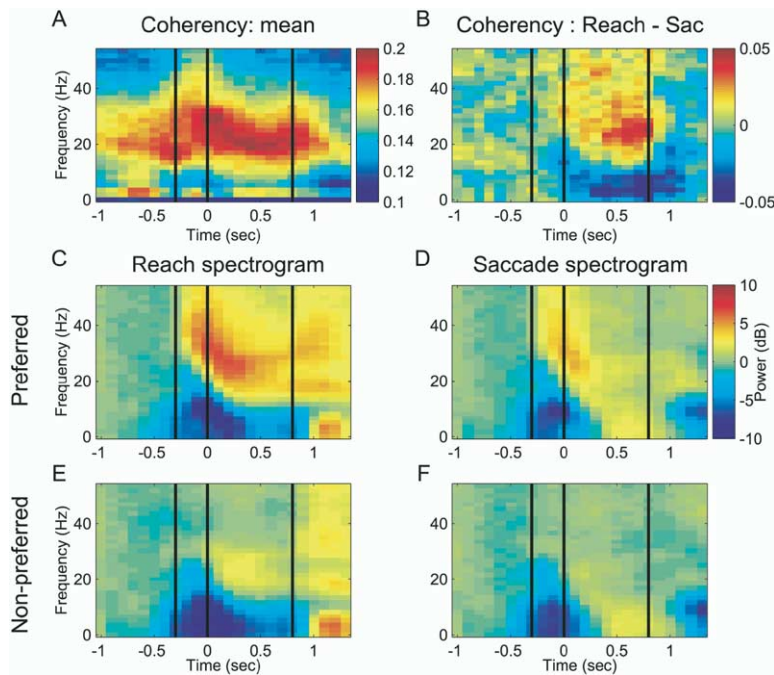


Figure 3. Population Coherograms and Spectrograms

(A and B) Population coherograms of the spike-field coherency. Color code indicates the mean coherency (A) and differential coherency (B) between the reach and saccade task.

(C–F) Population spectrograms of the LFP during the reach (C and E) and the saccade task (D and F) in the preferred (C and D) and the nonpreferred direction (E and F) of the LFP sites. Color code (in [D]) indicates the LFP power relative to the baseline spectrum (in dB). Vertical lines mark the beginning of the cue, planning, and movement period, respectively.

dicted the behavioral state of the animal on a trial-by-trial basis from the resulting population activity using a Bayesian classifier (see [Experimental Procedures](#)). We found that the correct behavioral state of the animal can be decoded from LFP signals on a trial-by-trial basis with an error rate of 10% or less using about 20 randomly selected recording sites ([Figure 2E](#)). In contrast, about 50 recording sites were necessary to achieve the same accuracy using spiking activity. These results indicate that LFP signals are better suited than spiking activity to predict the behavioral state of the animal and that PRR processes neural information in an action-specific fashion.

The action-specific nature of neural processing in PRR was also observed in the spike-field coherency between the LFP and spiking activity. [Figure 3A](#) presents the *mean* coherence across the reach and saccade conditions in the population of 137 recording sites. LFP and spiking activity for reaches and saccades were significantly coherent at mid frequencies (10–40 Hz) throughout the task. In contrast, [Figure 3B](#) shows the *difference* between the reach and saccade coherence in the population. Differences emerged mainly in the planning period, where the spike-field coherency was significantly enhanced for reaches versus saccades in the frequency range of 20–40 Hz, while at low frequencies (0–10 Hz) the coherency for saccade planning was enhanced with respect to reaches. These findings provide further evidence that neural processing in PRR is different for the generation of reach and saccade movements.

Different temporal structure was also observed in the population spectrogram of the LFP ([Figures 3C–3F](#)). Each panel shows the LFP power relative to the baseline power during the reach task ([Figures 3C and 3E](#)) and the saccade task ([Figures 3D and 3F](#)), while the

movement was made to the preferred ([Figures 3C and 3D](#)) or nonpreferred direction ([Figures 3E and 3F](#)) at each recording site (preferred direction was determined by the tuning of the LFP power at 25–35 Hz; nonpreferred direction was taken as opposite to the preferred). All four panels show suppression of the LFP power at the end of the cue presentation (time 0) at lower frequencies (below 20 Hz). Both preferred and nonpreferred reach directions show elevated low-frequency activity during the reach execution and low-frequency suppression beginning at cue presentation and continuing into the planning period. For saccades, both directions show an initial low-frequency suppression and then enhancements during the planning period. In fact, the low-frequency behavior is the same for the preferred and nonpreferred directions but different for reaches and saccades. In contrast, at higher frequencies (above 20 Hz), there is pronounced activity during reaching to the preferred direction, starting during cue presentation, that drops in frequency and then persists into the planning period. This pronounced activity is directionally tuned and largely absent for reaches to the nonpreferred direction. A similar but much weaker directional tuning was also observed during the planning of saccades. Taken together, the LFP shows a clear directional modulation at high frequencies (above 20 Hz) in addition to the state differences of the LFP at low frequencies.

To further investigate the directional LFP coding properties in PRR, we examined the directional tuning of the LFP signals toward eight peripheral targets in the reach and saccade task and compared it with spiking activity. The top panel of [Figure 4A](#) shows a typical directional tuning curve of a single unit, in which the cell's firing rate during the reach planning period is plotted against the movement direction, while the fitted von

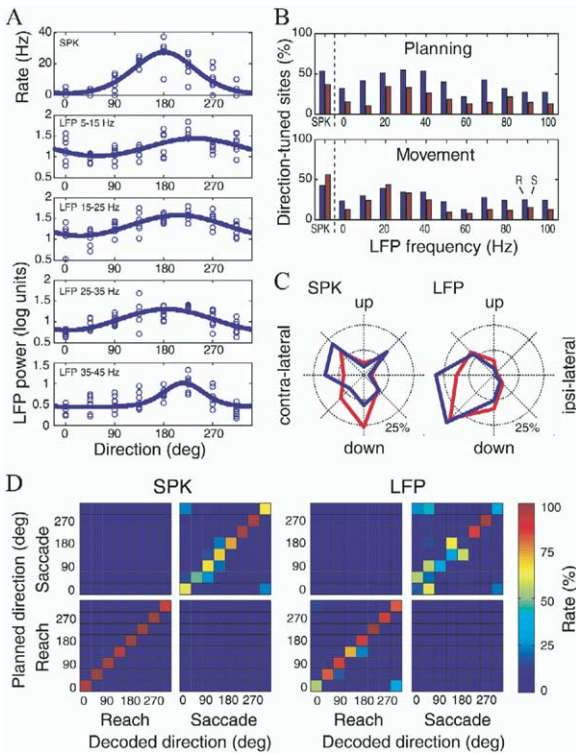


Figure 4. Direction Tuning of the LFP

(A) Typical recording site during reach planning. Each panel shows a tuning curve for spiking activity and in four LFP frequency bands (5–15, 15–25, 25–35, and 35–45 Hz). Circles denote the LFP power during individual trials, and thick curves are fitted von Mises distributions.

(B) Population results. Percentage of sites with significant directional tuning ($p < 0.05$) is shown for spiking activity (SPK) and 11 LFP frequency bands (0–100 Hz) during reach (blue bars) and saccade (red bars) planning and movement.

(C) Distribution of preferred directions of all tuned spiking activity (SPK) and all tuned LFP frequency bands during reach planning (blue) and saccade planning (red) with respect to the recorded hemisphere. Inner circle denotes uniform distribution.

(D) Decoding predictability of reach and saccade directions during movement planning using a Bayesian classifier. For comparison, confusion matrices are shown for spiking activity (SPK) and the LFP. Color code indicates the percentage of correct classifications (chance level 6.25%). 0° represents the ipsilateral, and 180° represents the contralateral planning direction.

Mises distribution (thick curve) indicates significant directional tuning ($p < 0.05$; preferred direction 181°) (Fischer, 1993). The panels below show the tuning of the LFP power for this recording site during reach planning for the frequencies 5–15, 15–25, 25–35, and 35–45 Hz. The LFP power was tuned in all of these frequency bands ($p < 0.05$; von Mises fit) with similar preferred directions of 238°, 207°, 185°, and 216°, respectively. These results were confirmed in the population analysis (Figure 4B). During reach planning, about 47% of all LFP signals were significantly tuned (blue bars) at frequencies between 5 and 55 Hz, while spiking activity was direction tuned at 53% of all recorded sites ($p < 0.05$; von Mises fit). The coefficient of determination (r^2 value), a measure of goodness of fit, had a mean of

0.40 for spikes and 0.23 for the LFP across significant fits in the population ($p < 0.05$), suggesting that the LFP conveys more information than spiking activity that is unrelated to the planned movement direction. A substantial number of recording sites were also tuned for saccade planning (red bars), which was demonstrated previously for spiking activity but not for the LFP (Snyder et al., 2000). Similar results were found for the movement period (Figure 4B, lower panel).

The distribution of preferred directions for the LFP as for spiking activity was biased toward the contralateral hemisphere during movement planning (Figure 4C) and movement execution (data not shown). This bias may reflect a contralateral preference of space representation in PRR (Snyder et al., 1997). However, a substantial number of PRR cells do code for ipsilateral space, consistent with a previous study (R. Quiñero et al., 2003, Soc. Neurosci., abstract).

To compare the coding information for movement direction in the LFP and in spiking activity, we simulated the decoding of the planned reach and saccade directions. Similar to the decoding of behavioral states, we treated our data set of sequentially recorded sites as if acquired simultaneously. To reduce noise, only neurons and those LFP frequency bands of each site were considered that presented significant directional tuning either for reaches or saccades (as shown in Figure 4B). This led to a population of 89 neurons and a population of 660 frequency bands from 125 LFP sites (57, 58, 86, 80, 79, 56, 41, 66, 54, 43, and 40 sites in the frequency bands of Figure 4B, respectively). The planned reach or saccade direction was then predicted from single trials of the population activity using a Bayesian classifier (see Experimental Procedures). We found that reach directions were predicted correctly in 81.4% of all simulations (range across directions, 53.7–98.9%) from our LFP population and in 97.3% (91.9%–100.0%) of all simulations from the spiking activity population (Figure 4D). The planned saccade direction was correctly classified in 40.1% (12.9%–96.6%) of all LFP simulations and in 72.2% (47.9%–98.2%) of all simulations using spiking activity. In general, classification rates were better for contralateral (135°–225°) than ipsilateral targets (–45°–45 deg°), which reflects the contralateral preference both for spiking activity (reach, 98.3% contralateral, 95.7% ipsilateral; saccade, 80.6% contralateral, 57.5% ipsilateral) and the LFP in this data set (reach, 86.8% contralateral, 72.2% ipsilateral; saccade, 42.0% contralateral, 22.8% ipsilateral). Misclassifications occurred mostly to neighboring directions, and reach and saccade plans were never confused, which is in line with our state decoding results (Figure 2E). This analysis indicates that spatial information for movement planning can be retrieved from LFP signals on a trial-by-trial basis. For both spikes and LFPs, performance was better for decoding reaches compared to saccades. While the encoding of the movement type was better represented in the LFP than in spiking activity (Figure 2E), spatial information of the planned movement direction was better represented in the spike data, consistent with the larger variance of the LFP signals for direction tuning.

Discussion

This study is, to our knowledge, the first examination of the temporal structure of LFP activity in PRR and its relation to spiking activity. Very pronounced differences in temporal structure were found that correlated with the behavioral state of the animals, including the type of movement, saccade or reach, that the monkeys were planning or executing. In fact, it was easier to determine the behavioral state from the LFPs than from spiking activity. The direction of planned movements is encoded in the LFPs, although the decoding of direction is better for spikes than LFPs. Spike activity is coherent with the LFPs and shows a greater degree of coherence for reach planning than for saccade planning. Additionally, the high-frequency (greater than 20 Hz) LFP power is greater when the monkeys are planning reaches compared to saccades. These findings provide new and additional evidence that the PPC is involved in movement planning (Snyder et al., 1997; Andersen and Buneo, 2002). The rich information contained in the LFP temporal structure can potentially provide a source of control signals for neural prosthetics that operate artificial limbs and other assistive devices, especially considering the ease and longevity of LFP recordings.

State and Direction Decoding

We found a larger predictability for the movement type with the LFP than with spiking activity, while the movement direction was better predicted by spiking activity than with the LFP. This difference may in part be due to the fact that LFPs cannot be simply interpreted as averaged spiking activity, but instead largely represent the mean dendritic activity within a cortical volume that results from synaptic input into the area as well as inter-neuronal activity (Buzsaki and Draguhn, 2004; Logothetis et al., 2001; Logothetis and Wandell, 2004). Since the generation of action potentials from synaptic input activity is a nonlinear process, LFPs provide an important alternative view at the neuronal input level that cannot be provided by spiking activity. Spiking activity is often sampled from larger cells in a cortical area that are cortical output neurons. Spiking and the LFP activity could therefore convey complementary information about the neuronal processing of a cortical area. This division is supported by our findings. The fact that the behavioral states are better encoded in the LFP than in spiking activity may indicate that the behavioral state information is already present at the input and local processing stages in PRR. The finding that the movement direction is better encoded in the spiking activity may be attributed to neural processing at the local and output stages of PRR.

It was observed that directional information for saccades, a different type of motor action, was encoded in the spiking activity with significantly less predictive power than for reaches. This result indicates a strong modulation for the type of action on the encoding of movement direction. Such a modulation by movement intention might use similar mechanisms seen for attention modulation in visual cortex, where a mechanism has been proposed that causes stimulus facilitation by increased synchronization of local cell assemblies

(Fries et al., 2001; Salinas and Sejnowski, 2000). In other words, increased synchronization of synaptic activity during reach planning, reflected in the LFPs, may lead to higher rates of spiking activity.

LFP activity at higher frequencies (15–40 Hz) is action and direction selective most prominently during the cue and planning periods of the task (Figures 3C–3F). These signals are most likely related to movement planning and working memory. In contrast, LFP activity at lower frequencies (0–15 Hz; Figures 3C–3F) is less direction selective and changes its spectral signature around the start of the movement (though differently for reaches and saccades). A possible role of these low-frequency signals may be to convey timing information, as also suggested for the low-frequency components of the LFP in the lateral intraparietal area (Pesaran et al., 2002). Whether these signals trigger or perhaps suppress a motor response needs further investigation.

Intention versus Attention

Spiking activity of the PPC has been implicated in action planning and spatial attention (Buneo et al., 2002; Colby and Goldberg, 1999; Goodale and Milner, 1992; Mountcastle et al., 1975; Robinson et al., 1978). It has been proposed by some investigators that the PPC only functions in spatial attention and does not have any role in movement planning (Bisley and Goldberg, 2003; Bushnell et al., 1981; Colby and Goldberg, 1999; Goldberg et al., 2002; Goldberg et al., 1990; Gottlieb and Goldberg, 1999; Gottlieb et al., 1998; Powell and Goldberg, 2000; Robinson et al., 1978). This strong claim is difficult to reconcile with the finding that the lateral intraparietal area within the PPC is more active when monkeys plan saccades, and less active when they plan reaches, whereas spiking activity in PRR shows the opposite behavior, being more active for reaches than saccades (Snyder et al., 1997). This double dissociation makes it unlikely that attentional load between reaches and saccades could be an explanation, especially considering that these two areas are so similar in terms of spatial representation and processing mechanisms other than those related to the type of action (Batista et al., 1999; Gnadt and Andersen, 1988).

The present study provides new, additional evidence for a role of the PPC in movement planning. First, the temporal profile of the LFPs in PRR is very different when animals are planning saccades and reaches to the same target. Most notably, there is a dramatic decrease in the below 10 Hz spectral component and increase in the above 10 Hz component during reach planning, whereas there is only a modest increase across the entire 1–100 Hz spectrum for saccade planning. Second, the power in the higher (above 20 Hz) direction-tuned LFP spectrum is substantially larger for reaches than saccades. Third, when adjusted for spike activity, spikes and local fields in PRR are more coherent when the animals are planning reaches compared to saccades. Finally, predicting the planned reach direction from the LFP is more robust than predicting saccade directions, again consistent with a degree of specialization of PRR for reach planning. If PRR activity is only related to attention, then these clear differences

would not be expected, since only the type of movement is varied in the experimental design. These data show that the LFP activity in PRR is intention specific, adding further evidence for the involvement of the PPC in movement planning.

Neural Prosthetic Applications

While the cortical mechanisms that generate coherent oscillations in the LFP need to be explored more extensively, it is apparent that cortical LFP signals are suitable for decoding movement intentions, e.g., as necessary for neuroprosthetic applications. A practical advantage to using LFPs compared to spikes is that they are easier to record and remain stable for longer periods of time. Both these features are due to the larger “listening sphere” of LFPs. Recording spikes is difficult in chronic implants, since the electrodes must be near the cell producing the spikes, whereas the LFP is a local average of cells over greater distances. Additionally, scarring that results from implants in time leads to a loss of signal from single neurons (Kralik et al., 2001; Rousche and Normann, 1998) but does not appreciably reduce the LFP signals. From an information point of view, using both spikes and LFPs will improve the amount and quality of information that can be decoded, because they largely reflect different aspects of neural processing. For instance, in the current experiments the behavioral state was better recovered with LFPs, and the direction of the movement plan was better recovered with spikes. The ability to use LFPs is likely to extend to most cortical regions; for instance, the direction of eye movements and behavioral state for planning and executing saccades have been decoded from the lateral intraparietal area, and the direction of reach movements has been decoded from motor cortex (Mehringer et al., 2003; Pesaran et al., 2002). Thus, the use of LFPs for neural prosthetics has the potential for extracting a wide variety of cognitive variables from a number of cortical regions.

Experimental Procedures

Animal Preparation

Two male rhesus monkeys (*Macaca mulatta*) participated in this study (animals C and D). Under sterile conditions, a stainless steel or titanium head post, a dental acrylic head cap, and a left or right recording chamber were implanted onto the skull (right hemisphere of animal C, both hemispheres of animal D). In addition, a scleral search coil was implanted under the conjunctiva of one eye in each animal (Judge et al., 1980; Scherberger et al., 2003b). Procedures followed federal guidelines and were approved by the local institutional animal care and use committee (National Research Council, 2003).

Animals were trained to touch buttons (diameter 3.7 cm) that were placed on a board in front of the animal at a distance of 26 cm. Each button contained a red and a green light-emitting diode (LED). The red LED instructed the animals where to look and maintain fixation, while the green LED instructed the animals where to place their hand. Reach movements were made with the contralateral arm, and eye position was monitored using the scleral search coil technique.

In the *delayed reach task*, the animal first fixated and touched a central fixation spot for a period of 800 ms (baseline period) before a green LED (visual cue) was presented for 300 ms at one of eight possible target positions. During the following delay period of 800 ms, the animal could plan to reach to the target but had to withhold

the execution until the central fixation light was extinguished. The animal then reached in the dark to the target while keeping its gaze at the (extinguished) central fixation spot. After pressing the target button for 500 ms, the animal was given a juice reward. In the similar *delayed saccade task*, a red LED was presented, which indicated to the animal to look at the target while keeping its hand at the central fixation button after the fixation light was extinguished in order to receive a juice reward.

Spiking (single-unit) activity and LFP activity were recorded simultaneously from a single varnished tungsten electrode (impedance 1–2 MΩ at 1 kHz; Frederick Haer Co.). Spiking activity was isolated from the amplified and filtered (0.6–6.0 kHz) signal using a time-amplitude window discriminator (Bak Electronics Inc.) and sampled at 2.5 kHz. LFP activity was digitized at 1000 Hz after being amplified and band-pass filtered (2–300 Hz) using a dedicated ac-differential amplifier and head stage (Bak Electronics Inc.).

Simultaneous spiking and LFP activity were recorded sequentially from a total of 137 recording sites (animal C: right hemisphere, 41; animal D: left hemisphere, 43; right hemisphere, 53). For state decoding, analysis was restricted to a subset of 119 sites that had at least 40 trials in each state condition. The approximate center of the PRR recording sites was 8 mm posterior and 5 mm lateral of stereotaxic zero (Horsley-Clarke coordinates) at depths below the superficial cortex (Buneo et al., 2002; Scherberger et al., 2003a). The correct position of the recording chambers above PRR was confirmed with MR images in one animal (D).

Data Analysis

Trials were aligned to the beginning of the delay period (cue offset). For spiking activity, peristimulus time histograms were generated using a Gaussian kernel (standard deviation 50 ms) and 95% confidence limits calculated by estimating the standard error of the mean.

Directional tuning of neuronal activity was fitted with a scaled and shifted version of the circular von Mises distribution:

$$y = a + b \frac{1}{2\pi I_0(\kappa)} e^{\kappa \cos(x - \theta)}$$

where the activity y is determined by the movement direction x and the four parameters: preferred direction θ , tuning width κ , vertical scale b , and offset a . The scaling factor $I_0(\kappa)$ is derived from the modified Bessel function of the first kind (Fischer, 1993). As a measure of the goodness of the fit, the coefficient of determination (r^2 value) was computed as: $r^2 = SS_{regression}/SS_{total}$, where $SS_{regression}$, SS_{total} denotes the sum of squares of the regression and the raw data, respectively (Zar, 1999).

To estimate the temporal structure in the LFP and the spike-field coherency, we applied multitaper spectral analysis that has been described extensively elsewhere (Jarvis and Mitra, 2001; Percival and Walden, 1993; Pesaran et al., 2002). In short, a Fourier transform was applied to the tapered time series signal. We used an optimal family of orthogonal tapers, the prolate spheroidal (Slepian) functions that are parameterized by their time length T and the frequency bandwidth W . For each choice of T and W , a maximal number of $K = 2TW - 1$ tapers can be used for spectral estimation.

The Fourier transform of the continuous valued LFP time series x_t , $t = 1, \dots, N$ (N the number of samples in the time window) is then given by $\bar{x}_k(f) = \sum_{t=1}^N w_t^{(k)} x_t e^{-2\pi i f t}$, with the K orthogonal taper functions $w_t^{(k)}$, $k = 1, \dots, K$. For the sequence of spike events t_j , $j = 1, \dots, N$ in the interval $[0, T]$, the windowed Fourier transform of the spike counts $\bar{x}_k(f)$ is given by

$$\bar{x}_k(f) = \sum_{j=1}^N w_{t_j}^{(k)} e^{-2\pi i f t_j} - N/T \bar{w}_0^{(k)}$$

where N denotes the total number of spikes in the window, and $\bar{w}_0^{(k)}$ denotes the Fourier transform of the data taper at zero frequency. For continuous and counting processes, the multitaper estimates of the spectrum $S_x(f)$, the cross-spectrum $S_{xy}(f)$, and the

coherency $C_{XY}(f)$ are then given by $S_x(f) = 1/K \sum_{k=1}^K |\bar{x}_k(f)|^2$, $S_{XY}(f) = 1/K \sum_{k=1}^K \bar{y}_k(f) \bar{x}_k^*(f)$, and $C_{XY}(f) = S_{XY}(f) / \sqrt{S_X(f)S_Y(f)}$. When averaging over several trials, an index i denoting the trial number is introduced, $\bar{x}_{k,i}(f)$, and averaging in the equations above is taken over all pairs k, i .

Error bars of multitaper spectrum and coherency estimates were generated using the jackknife method for single site analysis, and line noise was removed using an F test (Percival and Walden, 1993). Error bars in the population spectra indicate the standard error of the mean of the individual estimates of each site.

To estimate the discriminability of reach and saccade task spectra, a discriminability coefficient (dc) was defined as $dc = 1/F_{\max} \int_0^{F_{\max}} |S_{reach}(f) - S_{sac}(f)| df$, where $S_{reach}(f)$, $S_{sac}(f)$ denote the LFP log power spectrum (in dB) of the reach and saccade task, respectively, and $F_{\max} = 100$ Hz. To determine the significance of dc against the null hypothesis of identical reach and saccade spectra, a Monte Carlo method was employed that generated a null distribution of dc from randomly reshuffled data (10^4 repetitions in which each trial was randomly assigned to be a reach or saccade trial), from which the significance level for $p = 0.001$ was determined.

Decoding

A Bayesian classifier with uniform prior probability distribution was employed to estimate the behavioral states and the movement planning directions. For the decoding simulation, the sequentially recorded database was treated as if recorded simultaneously (Shenoy et al., 2003). We assumed Poisson spike statistics for the spiking activity, the log spectrum to be normally distributed in each of the 11 considered frequency bands of the LFP (0–5 Hz, 5–15 Hz, ..., 95–105 Hz), and statistical independence between different recording sites and between different LFP frequency bands at each site.

To estimate the behavioral states of the animal (baseline, reach planning, saccade planning, reach execution, or saccade execution), we defined the scalar $x \in \{1, \dots, 5\}$ to denote the state. The vector $\mathbf{a} = (a_1, \dots, a_M)$ represents the neural activity of the ensemble of all recording sites. In the case of spiking activity, M equals the number of recording sites, and each a_i represents the spike count of the i^{th} recording site. For the LFP, each a_i represents the LFP log power in one of 11 frequency bands. This leads to a vector of size 11 times the number of recording sites. Bayes' rule gives the following expression for the conditional probability of x given \mathbf{a} :

$$P(x|\mathbf{a}) = C(\mathbf{a}) P(x) \prod_{i=1}^M P_i(a_i|x),$$

where P_i is the distribution of a_i (Poisson for spikes and normal for the LFP), and $C(\mathbf{a})$ is a normalization factor that ensures the sum of all probabilities to be one. $P(x)$ is the prior probability, which is uniform by design. The estimated behavioral state \hat{x} was then taken to be the one with the highest likelihood:

$$\hat{x} = \underset{x}{\operatorname{argmax}} (P(x|\mathbf{a})).$$

Cross-validation was used to assess the performance of the estimation process. For each repetition of the simulation, a random subset of the total number of sites was selected, and one trial was randomly selected from each of the selected sites and set aside as test data. In the case of spiking activity, the parameter λ of the Poisson distribution was estimated from the mean firing rate in the remaining trials for each site and behavioral state condition. In the case of the LFPs, the remaining trials were used to estimate the mean and standard deviation of the LFP log power, which were then taken as the parameters μ and σ of the normal distribution. After all probability distributions P_i were estimated, $P(x|\mathbf{a})$ was determined for each state x using the test data \mathbf{a} , and the most probable state was selected as the prediction of a particular repetition. This process was repeated 100 times in each of the five behavioral states and for each tested number of sites.

The same method was applied for the decoding of the planning directions, where the scalar $x \in \{1, \dots, 16\}$ denoted the 8 + 8 possible reach and saccade directions, and 1000 repetitions per direction were done during cross-validation.

Acknowledgments

We thank B.G. Grieve, K. Pejsa, and L. Martel for animal care; T. Yao and C. Marks for administrative assistance; V. Shcherbatyuk for technical support; and C.A. Buneo and B. Pesaran for valuable comments on an earlier draft of this paper. This work was supported by the Christopher Reeve Paralysis Foundation, the James G. Boswell Foundation, DARPA, ONR, the Sloan-Swartz Center for Theoretical Neurobiology at Caltech, and the National Eye Institute.

Received: November 18, 2004

Revised: January 31, 2005

Accepted: March 4, 2005

Published: April 20, 2005

References

- Andersen, R.A., and Buneo, C.A. (2002). Intentional maps in posterior parietal cortex. *Annu. Rev. Neurosci.* 25, 189–220.
- Andersen, R.A., Snyder, L.H., Bradley, D.C., and Xing, J. (1997). Multimodal representation of space in the posterior parietal cortex and its use in planning movements. *Annu. Rev. Neurosci.* 20, 303–330.
- Andersen, R.A., Burdick, J.W., Musallam, S., Scherberger, H., Pesaran, B., Meeker, D., Corneil, B.D., Fineman, I., Nenadic, Z., Branchaud, E., et al. (2004). Recording advances for neural prosthetics. Paper presented at: Proceedings of the 26th Annual International Conference of the IEEE IMBS (San Francisco, CA).
- Batista, A.P., Buneo, C.A., Snyder, L.H., and Andersen, R.A. (1999). Reach plans in eye-centered coordinates. *Science* 285, 257–260.
- Bisley, J.W., and Goldberg, M.E. (2003). Neuronal activity in the lateral intraparietal area and spatial attention. *Science* 299, 81–86.
- Buneo, C.A., Jarvis, M.R., Batista, A.P., and Andersen, R.A. (2002). Direct visuomotor transformations for reaching. *Nature* 416, 632–636.
- Bushnell, M.C., Goldberg, M.E., and Robinson, D.L. (1981). Behavioral enhancement of visual responses in monkey cerebral cortex. I. Modulation in posterior parietal cortex related to selective visual attention. *J. Neurophysiol.* 46, 755–772.
- Buzsaki, G. (2004). Large-scale recording of neuronal ensembles. *Nat. Neurosci.* 7, 446–451.
- Buzsaki, G., and Draguhn, A. (2004). Neuronal oscillations in cortical networks. *Science* 304, 1926–1929.
- Colby, C.L., and Goldberg, M.E. (1999). Space and attention in parietal cortex. *Annu. Rev. Neurosci.* 22, 319–349.
- Engel, A.K., Konig, P., Gray, C.M., and Singer, W. (1990). Stimulus-dependent neuronal oscillations in cat visual cortex: Inter-columnar interaction as determined by cross-correlation analysis. *Eur. J. Neurosci.* 2, 588–606.
- Fischer, N.I. (1993). *Statistical Analysis of Circular Data* (Cambridge: Cambridge University Press).
- Fries, P., Reynolds, J.H., Rorie, A.E., and Desimone, R. (2001). Modulation of oscillatory neuronal synchronization by selective visual attention. *Science* 291, 1560–1563.
- Fromm, G.H., and Bond, H.W. (1964). Slow changes in the electrocorticogram and the activity of cortical neurons. *Electroencephalogr. Clin. Neurophysiol.* 17, 520–523.
- Gnadt, J.W., and Andersen, R.A. (1988). Memory related motor planning activity in posterior parietal cortex of macaque. *Exp. Brain Res.* 70, 216–220.
- Goldberg, M.E., Colby, C.L., and Duhamel, J.R. (1990). Representation of visuomotor space in the parietal lobe of the monkey. *Cold Spring Harb. Symp. Quant. Biol.* 55, 729–739.
- Goldberg, M.E., Bisley, J., Powell, K.D., Gottlieb, J., and Kusunoki, M. (2002). The role of the lateral intraparietal area of the monkey in the generation of saccades and visuospatial attention. *Ann. N Y Acad. Sci.* 956, 205–215.
- Goodale, M.A., and Milner, A.D. (1992). Separate visual pathways for perception and action. *Trends Neurosci.* 15, 20–25.

- Gottlieb, J., and Goldberg, M.E. (1999). Activity of neurons in the lateral intraparietal area of the monkey during an antisaccade task. *Nat. Neurosci.* 2, 906–912.
- Gottlieb, J.P., Kusunoki, M., and Goldberg, M.E. (1998). The representation of visual salience in monkey parietal cortex. *Nature* 397, 481–484.
- Gray, C.M., Konig, P., Engel, A.K., and Singer, W. (1989). Oscillatory responses in cat visual cortex exhibit inter-columnar synchronization which reflects global stimulus properties. *Nature* 338, 334–337.
- Jarvis, M.R., and Mitra, P.P. (2001). Sampling properties of the spectrum and coherency of sequences of action potentials. *Neural Comput.* 13, 717–749.
- Judge, S.J., Richmond, B.J., and Chu, F.C. (1980). Implantation of magnetic search coils for measurement of eye position: an improved method. *Vision Res.* 20, 535–538.
- Kralik, J.D., Dimitrov, D.F., Krupa, D.J., Katz, D.B., Cohen, D., and Nicolelis, M.A. (2001). Techniques for long-term multisite neuronal ensemble recordings in behaving animals. *Methods* 25, 121–150.
- Logothetis, N.K., and Wandell, B.A. (2004). Interpreting the BOLD signal. *Annu. Rev. Physiol.* 66, 735–769.
- Logothetis, N.K., Pauls, J., Augath, M., Trinath, T., and Oeltermann, A. (2001). Neurophysiological investigation of the basis of the fMRI signal. *Nature* 412, 150–157.
- Mehring, C., Rickert, J., Vaadia, E., Cardoso de Oliveira, S., Aertsen, A., and Rotter, S. (2003). Inference of hand movements from local field potentials in monkey motor cortex. *Nat. Neurosci.* 6, 1253–1254.
- Mitzdorf, U. (1987). Properties of the evoked potential generators: current source-density analysis of visually evoked potentials in the cat cortex. *Int. J. Neurosci.* 33, 33–59.
- Mountcastle, V.B., Lynch, J.C., Georgopoulos, A., Sakata, H., and Acuna, C. (1975). Posterior parietal association cortex of the monkey: command functions for operations within extrapersonal space. *J. Neurophysiol.* 38, 871–908.
- Murthy, V.N., and Fetz, E.E. (1996). Synchronization of neurons during local field potential oscillations in sensorimotor cortex of awake monkeys. *J. Neurophysiol.* 76, 3968–3982.
- National Research Council, E.E. (2003). *Guidelines for the Care and Use of Mammals in Neuroscience and Behavioral Research* (Washington, D.C.: National Academies Press).
- Percival, D.B., and Walden, A.T. (1993). *Spectral Analysis for Physical Applications—Multitaper and Conventional Univariate Techniques* (Cambridge, MA: Cambridge University Press).
- Pesaran, B., Pezaris, J.S., Sahani, M., Mitra, P.P., and Andersen, R.A. (2002). Temporal structure in neuronal activity during working memory in macaque parietal cortex. *Nat. Neurosci.* 5, 805–811.
- Powell, K.D., and Goldberg, M.E. (2000). Response of neurons in the lateral intraparietal area to a distractor flashed during the delay period of a memory-guided saccade. *J. Neurophysiol.* 84, 301–310.
- Robinson, D.L., Goldberg, M.E., and Stanton, G.B. (1978). Parietal association cortex in the primate: sensory mechanisms and behavioral modulations. *J. Neurophysiol.* 41, 910–932.
- Rousche, P.J., and Normann, R.A. (1998). Chronic recording capability of the Utah Intracortical Electrode Array in cat sensory cortex. *J. Neurosci. Methods* 82, 1–15.
- Salinas, E., and Sejnowski, T.J. (2000). Impact of correlated synaptic input on output firing rate and variability in simple neuronal models. *J. Neurosci.* 20, 6193–6209.
- Sanes, J.N., and Donoghue, J.P. (1993). Oscillations in local field potentials of the primate motor cortex during voluntary movement. *Proc. Natl. Acad. Sci. USA* 90, 4470–4474.
- Scherberger, H., and Andersen, R.A. (2003). Sensorimotor transformations. In *The Visual Neurosciences*, L.M. Chalupa and J.S. Werner, eds. (Cambridge, MA: MIT Press), pp. 1324–1336.
- Scherberger, H., Fineman, I., Musallam, S., Dubowitz, D.J., Bernheim, K.A., Pesaran, B., Corneil, B.D., Gillikin, B., and Andersen, R.A. (2003a). Magnetic resonance image-guided implantation of chronic recording electrodes in the macaque intraparietal sulcus. *J. Neurosci. Methods* 130, 1–8.
- Scherberger, H., Goodale, M.A., and Andersen, R.A. (2003b). Target selection for reaching and saccades share a similar behavioral reference frame in the macaque. *J. Neurophysiol.* 89, 1456–1466.
- Shenoy, K.V., Meeker, D., Cao, S., Kureshi, S.A., Pesaran, B., Buneo, C.A., Batista, A.P., Mitra, P.P., Burdick, J.W., and Andersen, R.A. (2003). Neural prosthetic control signals from plan activity. *Neuroreport* 14, 591–596.
- Siegel, M., and Konig, P. (2003). A functional gamma-band defined by stimulus-dependent synchronization in area 18 of awake behaving cats. *J. Neurosci.* 23, 4251–4260.
- Snyder, L.H., Batista, A.P., and Andersen, R.A. (1997). Coding of intention in the posterior parietal cortex. *Nature* 386, 167–170.
- Snyder, L.H., Batista, A.P., and Andersen, R.A. (2000). Saccade-related activity in the parietal reach region. *J. Neurophysiol.* 83, 1099–1102.
- Zar, J.H. (1999). *Biostatistical Analysis* (Upper Saddle River, NJ: Prentice-Hall).